BJRS
BRAZILIAN JOURNAL OF RADIATION SCIENCES

doi.org/10.15392/2319-0612.2024.2497
**2024, 12(4) | 01-23 | e2497**
Submitted: 2024-06-03
Accepted: 2024-08-21

# Study of CdTe detector response functions using different MCNPX computational modeling detailing

Antunes [a], A. M.; Mendes[a], B. M.; Squair [a], P. L.; Nogueira [a], M. S.; Almeida-Jr [b], A. T..; Lacerda[a*], M. A. S.

[a] Centro de Desenvolvimento da Tecnologia Nuclear, CDTN, Av. Presidente Antônio Carlos, 6627, Pampulha, CEP: 31270-901 Belo Horizonte, MG, Brazil.

[b] Fundação Jorge Duprat Figueiredo de Segurança e Medicina do Trabalho, FUNDACENTRO, Rua dos Guajajaras, nº 40, 13º e 14º andares, CEP: 30180100 - Belo Horizonte, MG - Brazil

*Correspondence: author_masl@cdtn.br; madslacerda@gmail.com

**Abstract**: The spectra measured with cadmium telluride (CdTe) detectors show high spectral distortions that must be corrected by applying a mathematical algorithm along with the detector's response functions. Simplified computational modeling of the CdTe detector is generally used to obtain its response functions. In this work, the Monte Carlo code MCNPX was used to study the response functions of a CdTe detector using more complex detector modeling and compared it with those obtained by simplified modeling. Raw spectra were corrected using the response matrices obtained for the simplified and detailed modeling of the CdTe and compared with those obtained with reference-validated software.

**Keywords:** X-ray spectra, Response function, CdTe detector, MCNPX.

SBPR

BJRS
BRAZILIAN JOURNAL OF RADIATION SCIENCES

doi.org/10.15392/2319-0612.2024.2497
**2024, 12(4) | 01-23 | e2497**
Submitted: 2024-06-03
Accepted: 2024-08-21

# Estudo das funções resposta do detector CdTe utilizando o código MCNPX com diferentes níveis de detalhamento da geometria

**Resumo**: Os espectros medidos com detectores de telureto de cádmio (CdTe) apresentam grandes distorções espectrais que devem ser corrigidas aplicando um algoritmo matemático juntamente com as funções de resposta do detector. A modelagem computacional simplificada do detector CdTe é geralmente usada para obter as funções de resposta. Neste trabalho, o código de Monte Carlo MCNPX foi utilizado para estudar as funções de resposta de um detector CdTe utilizando uma modelagem mais complexa e detalhada. Os resultados encontrados foram comparados com aqueles obtidos por modelagem simplificada. Os espectros brutos foram corrigidos utilizando as matrizes de resposta obtidas para a modelagem simplificada e detalhada do CdTe e comparados com aqueles obtidos com software validado por referência.

**Palavras-chave:** Espectro de raios X, Função Resposta, Detector CdTe, MCNPX.

SBPR

## 1. INTRODUCTION

Measurements of the energy spectra of X-ray equipment present two main difficulties. The first one is the high photon fluence rates which result in high dead time in the detection system. The second difficulty is the spectral distortion caused by the following factors: (a) random coincidences; (b) photon and/or electron escape effects from the detector's active volume; (c) phenomena associated with the transport of charge carriers in the detector volume, which can cause incomplete collection of the produced charges; and (d) effects related to the finite energy resolution of detection systems [1-3]. Radiation scattering in detector and collimator structures, absorption of low-energy photons in the input window, and penetration of high-energy photons through the collimation system also contribute to the distortions of the acquired spectra.

In recent years, portable cadmium telluride (CdTe) detectors have been widely used for spectral measurements in the radiodiagnostic energy range. These detectors have advantages such as high atomic number (which results in higher detection efficiency), small dimensions, operation at room temperature, and good energy resolution compared to scintillators [4]. However, the spectra measured with CdTe detectors show higher spectral distortions than those obtained with HPGe and Si(Li) detectors [2;3].

The knowledge of the detector response function (R(E)) is necessary to correct the spectra measured with CdTe [2]. The response function can be obtained by analytical, experimental, or Monte Carlo methods [1; 2; 5-10]. Once the response matrix of a detector as a function of energy is known, the spectrometric measurements can be corrected by applying a mathematical procedure called stripping [3; 11].

Several studies show the use of Monte Carlo codes to obtain response matrices for CdTe detectors [2; 3; 9; 10]. Simplified modeling of the CdTe detector, considering only the crystal, the beryllium window, and the electrodes, are generally employed.

The objective of the present work is to use the computational code based on the Monte Carlo method, MCNPX, to study the response functions of a CdTe detector using different detector modelling detailing. All detector components, including its collimation system, were carefully modeled. Then, the response functions were calculated and compared with those obtained by simplified modeling. Furthermore, raw spectra, obtained experimentally [12], were corrected using the response matrices obtained for the simplified and detailed modeling of the CdTe and compared with those obtained with a reference-validated software.

## 2. MATERIALS AND METHODS

The response functions of the CdTe semiconductor detector AmpTek® model EXV9 – XR-100T were obtained using the MCNPX code, version 2.7.0. Three types of modeling were done: (a) simplified (SIMP), which considers only the CdTe crystal, cathode, anode and Beryllium window; (b) complete without the collimator (CNC), which considers the maximum amount of information and constructive details of the detector made available by the manufacturer or in the literature and; (c) complete with the collimator (CWC), considering the CNC model coupled to the tungsten collimator with a hole diameter of 0.1 mm. Figure 1 shows the details of each model.

A circular source of photons with a diameter of 0.1 mm was positioned immediately above the beryllium window, perpendicularly incident on the CdTe crystal. The CdTe response matrix was constructed for photon energies ranging from 0 keV to 200 keV, with energy bins, E_bin, of 0.25 keV. This E_bin value was chosen by observing detector

calibrations in laboratory practice. System users reported E_bin values ranging from 0.20 to 0.30 keV, corresponding to the slope of the channel energy calibration curve. Simulation bins are analogous to detector channels. Therefore, the bins will be treated in this work as channels of the simulated detector. Thus, the modeled detector has 800 channels.

The response matrix was constructed for monoenergetic beams with energy, E_mono, equal to the central energy value of each channel of the modeled detector. Thus, the photopeak efficiency and undesirable pulses in the lower channels were calculated. One case was executed for each channel of the simulated detector, totaling 800 cases. MCNPX tally F8 was used to evaluate the energy distribution of photon pulses created in the CdTe crystal per photon emitted at the source in each simulated case [13].

The secondary transport of particles was evaluated using the electron and photon transport mode (MODE P E). The cross-section libraries MCPLIB04 [14] e EL03 [15] were used. The default cutoff energy for photons and electrons, 1 keV, was maintained. Sufficient stories were simulated to provide relative errors in photopeak counts (Tally F8) of less than 1 % [13].

Additionally, CWC simulations were performed using tally F8 together with a special treatment card, called GEB (Gaussian Energy Broadening), which seeks to adjust the photopeaks to a Gaussian function, similar to the spectrum obtained experimentally [16]. For this, three parameters (a, b, c) are used, which are related to the experimental FWHM and the energy, E, of the particle by Equation 1. The parameters a, b, and c are coefficients that must be calculated according to the measured $FWHM$ [13].

$$FWHM = a + b\sqrt{E + cE^2} \qquad (1)$$

In this work, the parameters a, b, and c of equation 1, defined by (Stankovic et al., 2015) [17] were used ($a = 2{,}0296 \cdot 10^{-4}\ MeV$, $b = 1{,}8 \cdot 10^{-3} MeV^{1/2}$ and $c = 0$).

**Figure 1:** Details of the three MCNPX modeling: (A) Simplified (SIMP), (B) Complete Without Collimator (CNC); (C) Complete With Collimator (CWC).

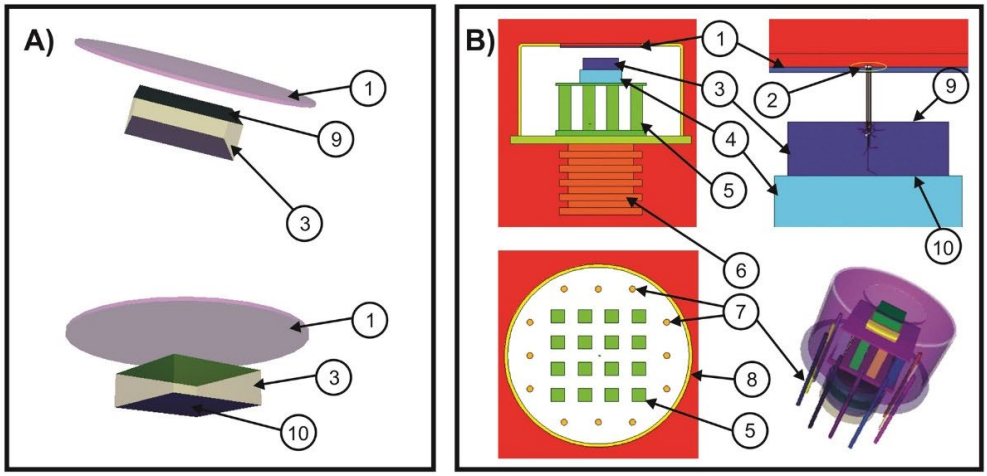


**1) Beryllium window; 2) Source; 3) CdTe crystal; 4) Crystal substrate; 5) Peltier cooler; 6) Bracket screew; 7) Copper Pins; 8) Nickel plating; 9) Platinum cathode; 10) Indium anode.**

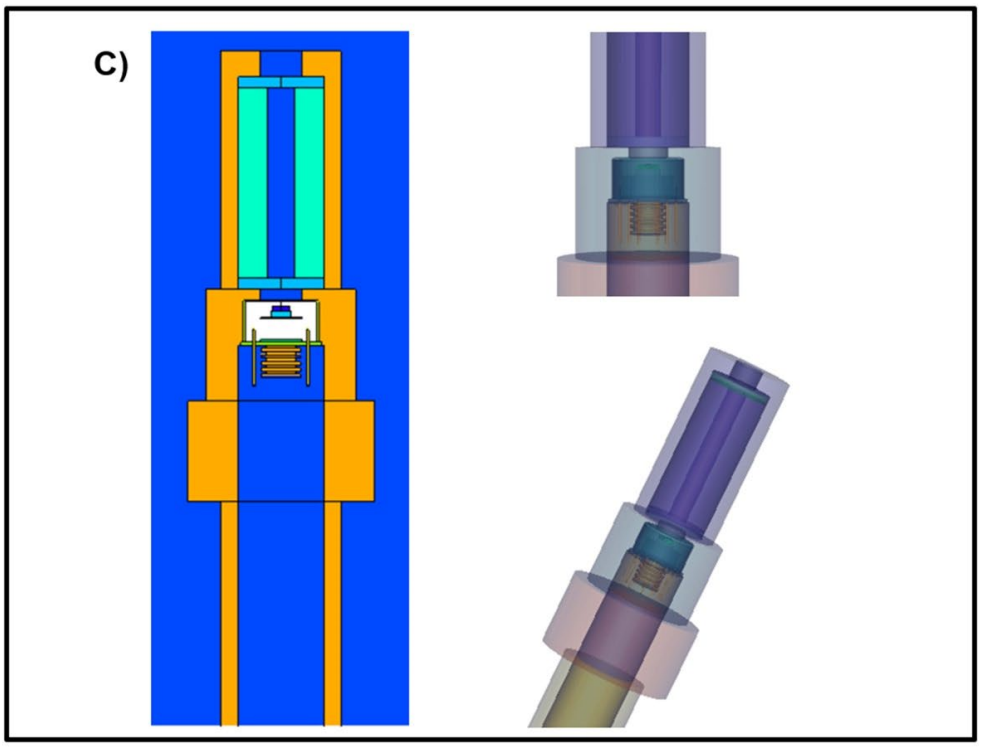


Raw spectra RQR10, W60, N80, N120, and W150 measured with a CdTe detector from the same manufacturer/model [12] were corrected using the different response matrices and compared with those corrected using the ADMCA (Amptek Inc. Bedford, MA,

USA) software, also used by Santos et al. (2017) [18]. Qualitative (visual) and quantitative (ratios between responses) comparisons were made between the corrected spectra. In addition, the mean energies of the spectra, the values of the first and second half-value layers (HVL), and the coefficient of homogeneity (h) were compared.

A C++ program developed in-house [19] was used to automate the striping procedure for spectra correction using the response matrix obtained. The corrections made with the response matrix obtained with the CWC model were compared with the corrections made with response matrices generated with the SIMP and CNC models.

The average energy, $E_{med}$, of the spectrum was calculated using equation 2.

$$E_{med} = \frac{\sum_{i=C_1}^{C_{max}} Cont_i \cdot E_i}{\sum_{i=C_1}^{C_{max}} Cont_i} \quad (2)$$

where, $Cont_i$ is the number of counts in the channel i of the spectrum; $\sum_{i=C_1}^{C_{max}} Cont_i$ is the total countings in all the channels (from the first, $C_1$, to the last, $C_{max}$); and $E_i$ is the maximum average energy of the channel $i$.

The value of the first HVL was calculated based on the work of [20]. According to this study, the value of the 1st HVL is given by the thickness, $x$, of attenuating material (aluminum or copper, in the spectra evaluated in this study) that satisfies the following relationship:

$$\sum_{i=C_1}^{C_{max}} Cont_i \cdot e^{-\mu_i x} = \frac{1}{2} \cdot \left( \sum_{i=C_1}^{C_{max}} Cont_i \right) \quad (3)$$

where, $\mu_i$ is the linear attenuation coefficient of the attenuating material obtained from XCOM/NIST [21] for the maximum energy of channel $i$. Likewise, the 2nd HVL was calculated using the same equation, replacing the counts, $Cont_i$, by the counts obtained after

an attenuating material thickness equal to 1 HVL. The Homogeneity Coefficient, *h*, is the quotient between the 1st HVL and the 2nd HVL.

## 3. RESULTS AND DISCUSSIONS

The response functions for monoenergetic photons of 50 keV and 160 keV, and the ratios between these functions obtained by simulating the three types of detector modeling: SIMP, CNC, and CWC, are presented in Figures 2-6.

**Figure 2:** Comparison between response function for 50 keV photons using CdTe detector modeling: simplified (SIMP), complete without collimator (CNC), and complete with a collimator (CWC). PP: photopeak; EP: escape peaks; CE: Compton Edge, and; CC: Compton Continuum region.

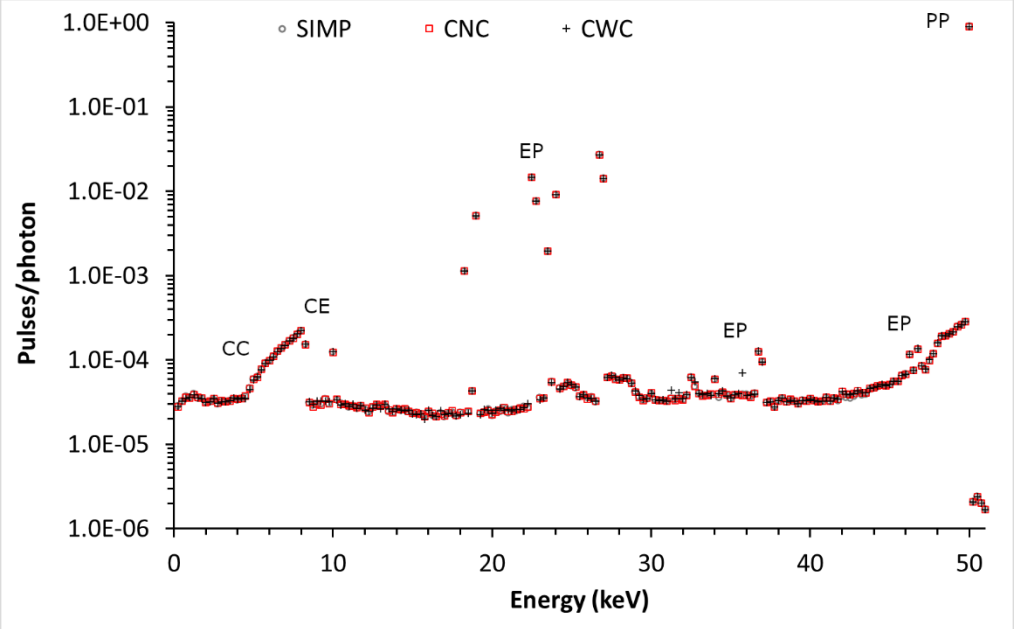

**Figure 3:** Ratios between the response functions obtained with SIMP, CNC, and CWC simulations for 50 keV energy photons.

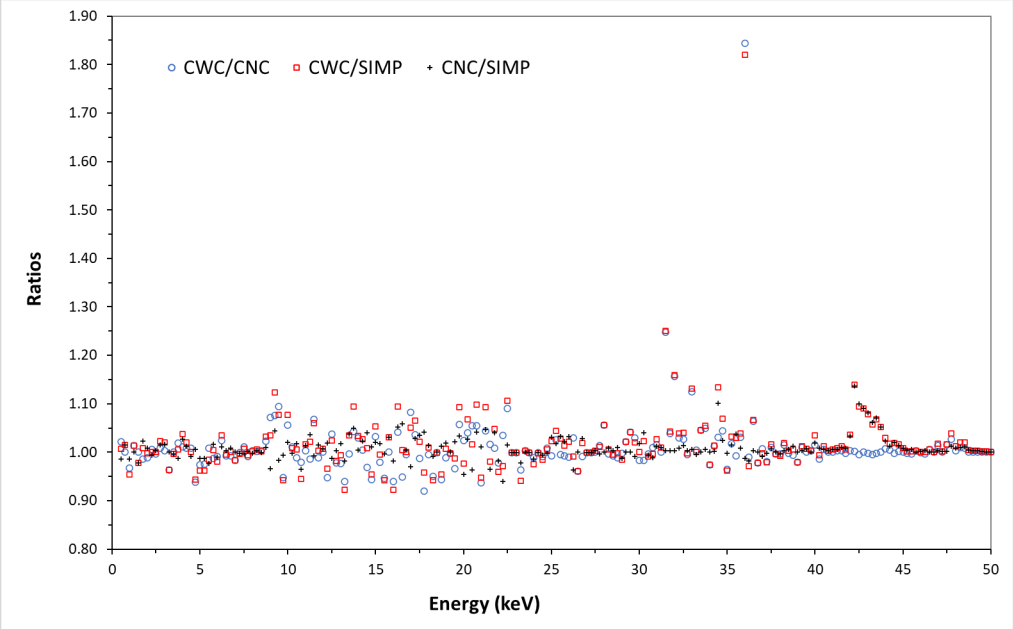


**Figure 4:** Comparison between the response function for 160 keV photons using CdTe detector modeling: simplified (SIMP), complete without collimator (CNC), and complete with collimator (CWC). PP: photopeak; EP: escape peaks; CE: Compton Edge; CC: Compton Continuum region, and; BS: backscattered photon pulses.

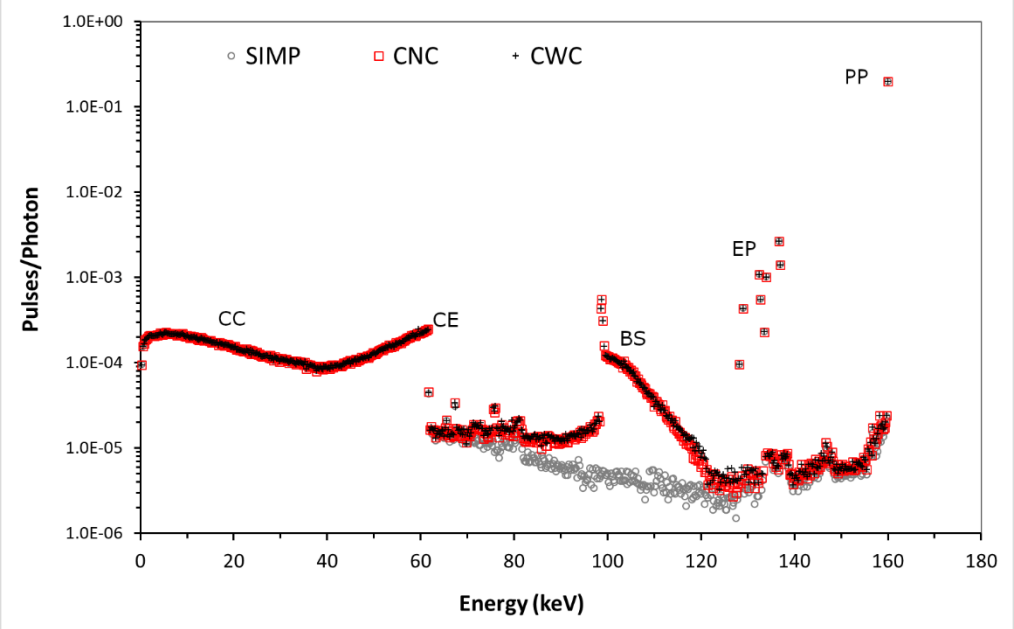

**Figure 5:** Ratio between SIMP, CNC, and CWC simulations for 160 keV energy photons.

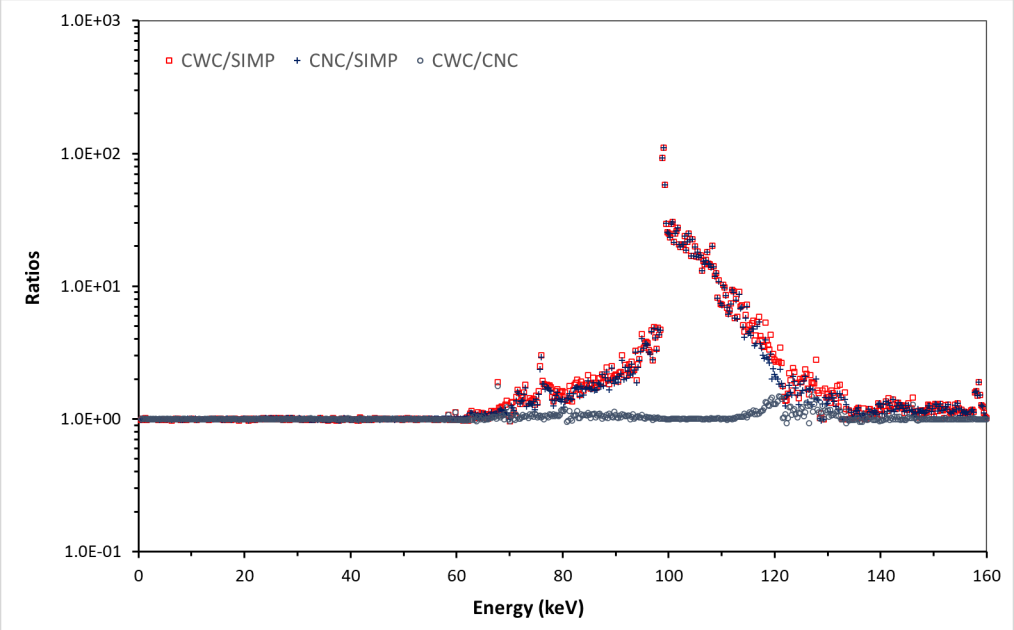


**Figure 6:** CWC/CNC ratio and CWC response function for 160 keV energy photons.

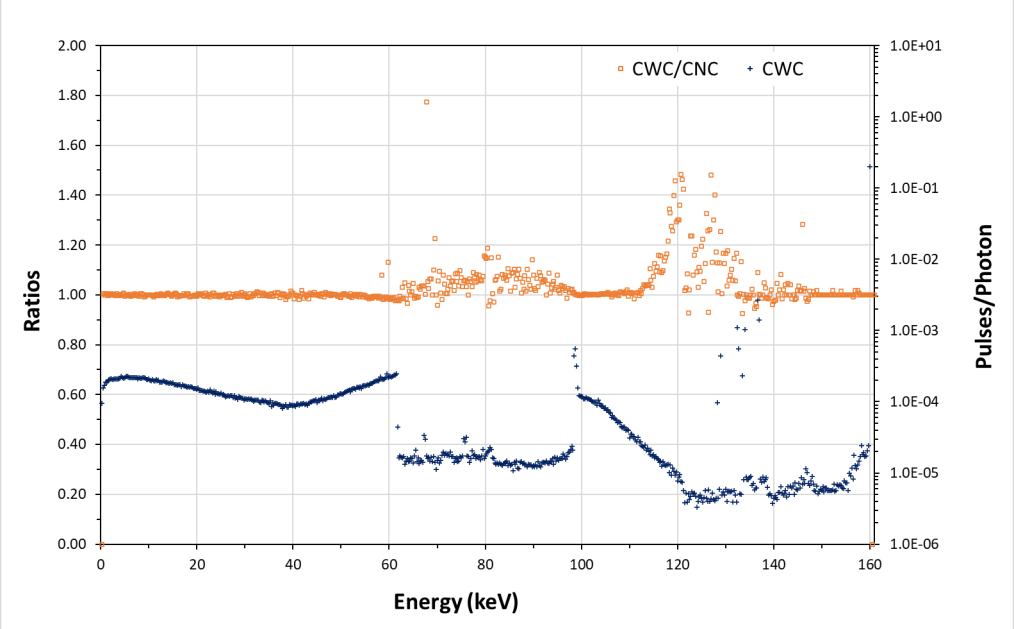


Figure 2 shows no significative visual differences between the response functions for 50 keV photons obtained for the three models. This fact can also be evidenced by observing

the ratios between the response functions, shown in Figure 3. The CWC/CNC ratios averaged 1.01, considering all channels. The minimum ratio was 0.92, and the maximum was 1.84. The average CWC/SIMP ratio was 1.02, and the minimum and maximum ratios were 0.92 and 1.82, respectively. For most complete modeling of the detectors (CWC and CNC), the main differences in the response function are due to the backscattered photons and characteristic x-rays originating from adjacent structures.

As the incident photon energy increases, the differences between the CWC and CNC simulations and the simplified modeling (SIMP) become more evident. In Figure 4, it can be observed that for CWC and CNC there is an increase in the number of counts in practically all channels with energy above the Compton Edge in relation to SIMP modeling. The CWC/SIMP and CNC/SIMP ratios, shown in Figure 5, more clearly portray these differences. For example, the average of the CWC/SIMP ratios considering all channels was 3.22, with the minimum ratio being 0.96 and the maximum 110.62.

When evaluating the CWC/CNC ratios, an average value of 1.03 is obtained when all channels are considered. However, as can be seen in Figure 6, in specific regions of the response function, the extra number of counts attributed to secondary radiation generated by the collimator structures is significantly higher. It is observed that in the range from 110 keV to 130 keV, there is a considerable increase (15 % on average per channel) in backscattering. In addition, it is possible to notice an average increase of 5.0 % in the channel counts located between the backscatter peak and the Compton threshold. The other region in which an average increase in counts in the CWC response function is observed about the CNC is located in the most energetic portion of the backscattering ramp. In the case of incident photons of 160 keV, this region comprises energies from 110 keV to 130 keV, and the average increase in counts per channel is about 15 %.

Simulation results indicate that for photons of lower energies such as those of 50 keV, the changes made in the modeling do not contribute significantly to the response curve of

the semiconductor crystal. However, for energies above 100 keV a more complex modeling can result in more realistic response functions and, therefore, in better spectral corrections.

Figure 7 shows a comparison between the simulated peak efficiency for the following models of detector: SIMP, CNC, CWC, and CWC with the use of GEB card.

**Figure 7:** Peak efficiency for the simulations of the following models of detector: SIMP, CNC, CWC, and CWC with the use of GEB card.

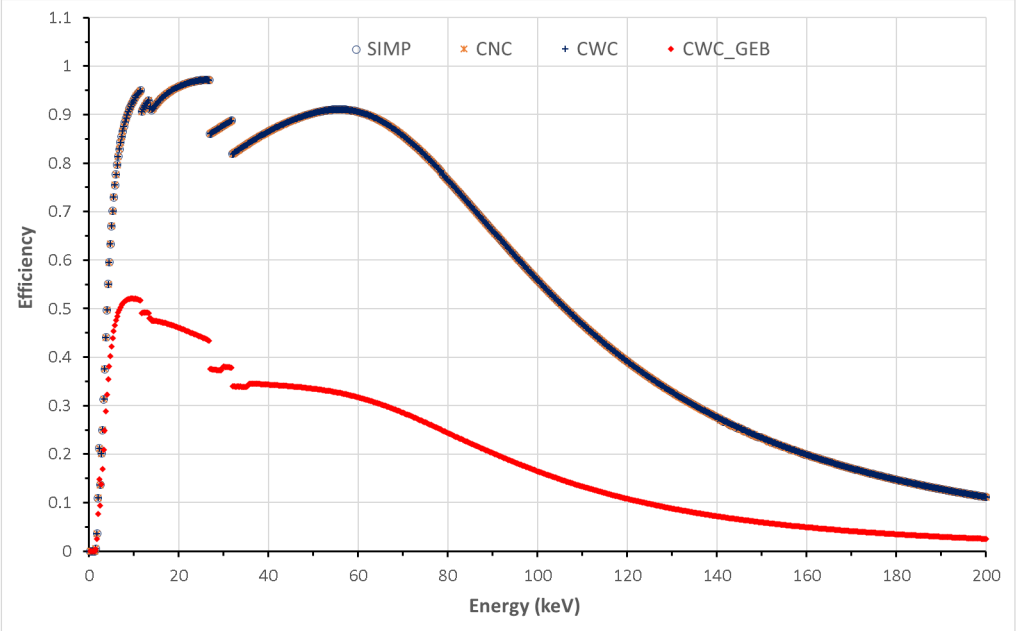


No significant differences were observed between the efficiencies for the models SIMP, CNC and CWC, with the greatest variations being observed in the range from 140 keV to 160 keV (maximum 0.75 %). The efficiencies calculated for the model CWC with the GEB card are always smaller than those calculated without this card (efficiencies were from 34% to 338% smaller than those calculated without GEB card). This is a characteristic of the mathematical algorithm, which seeks to adjust the photopeaks to a Gaussian function. As the peak efficiency is calculated considering the centroid channel of the peak, this Gaussian adjustment decreases the number of pulses in the centroid channel. If the peak efficiency is calculated considering five channels around the centroid, the differences virtually disappear.

Efficiencies for the simulations of the models of detector SIMP, CNC, and CWC present maximum value for energy 26.75 keV (K edge of Cd). It is also observed edges at energies 11.5 keV (L3-edge of Pt from cathode), 13.25 keV (L2-edge of Pt from cathode), and 31.75 keV (K edge of Te). The edges are as pronounced as greater are the emission probabilities. For the simulations with the GEB card, there are also the same edges. However, they are less abrupt, due to the broadening adjustment, given by the treatment with the GEB card, which smooths the curves.

Figures 8-11 show comparisons of the responses obtained with the CWC and CWC_GEB models for photons with 20 keV, 60 keV, 100 keV, and 160 keV photon energy.

**Figure 8:** Comparison of the responses obtained for photons with 20 keV using the CdTe detector modelling: complete with a collimator (CWC) and complete with a collimator and GEB card (CWC_GEB). PP: photopeak; EP: escape peaks; CE: Compton Edge, and; CC: Compton Continuum region.

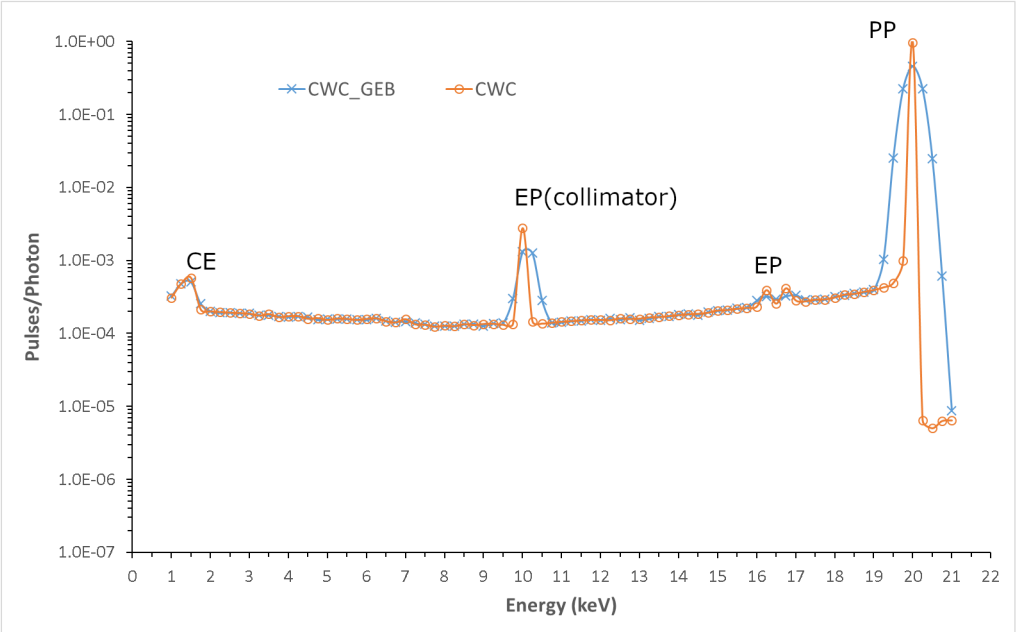

**Figure 9:** Comparison of the responses obtained for photons with 60 keV using the CdTe detector modelling: complete with a collimator (CWC) and complete with a collimator and GEB card (CWC_GEB). PP: photopeak; EP: escape peaks; CE: Compton Edge, and; CC: Compton Continuum region.

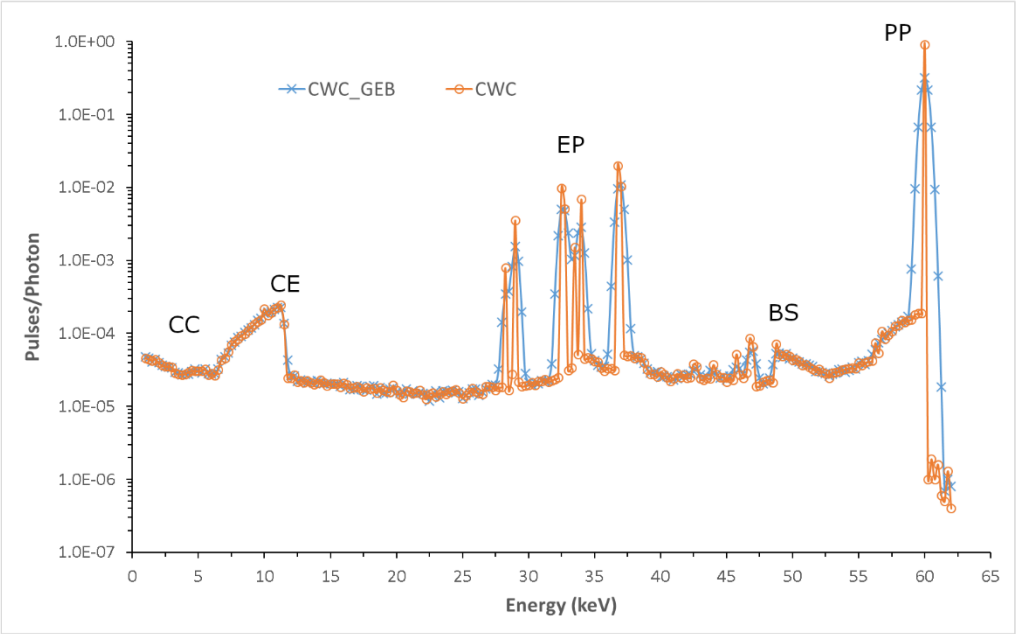


**Figure 10:** Comparison of the responses obtained for photons with 100 keV using the CdTe detector modelling: complete with a collimator (CWC) and complete with a collimator and GEB card (CWC_GEB). PP: photopeak; EP: escape peaks; CE: Compton Edge, and; CC: Compton Continuum region.

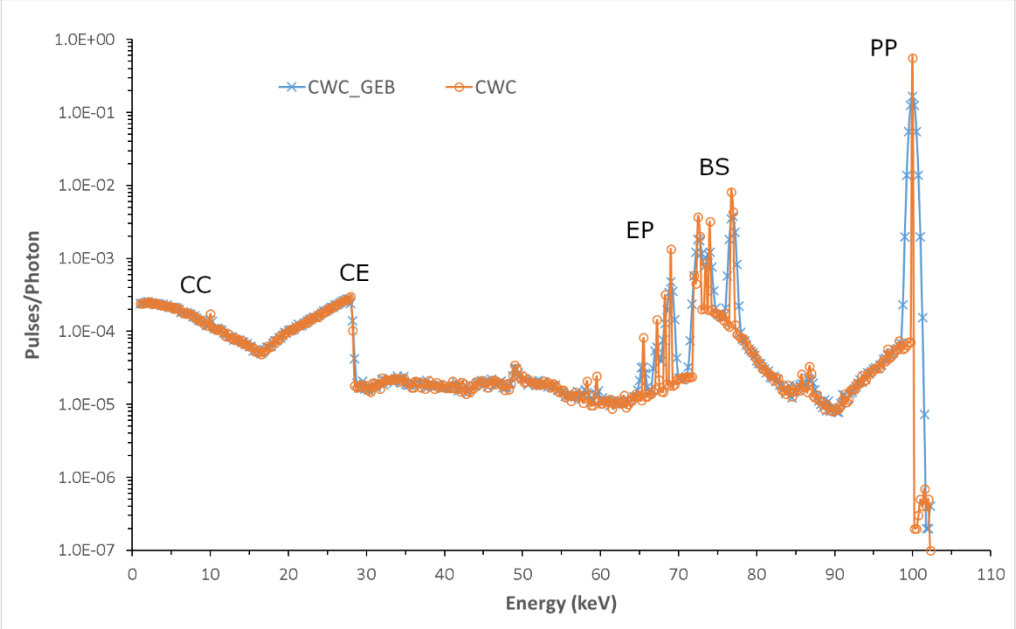

**Figure 11:** Comparison of the responses obtained for photons with 160 keV using the CdTe detector modelling: complete with a collimator (CWC) and complete with a collimator and GEB card (CWC_GEB). PP: photopeak; EP: escape peaks; CE: Compton Edge, and; CC: Compton Continuum region.

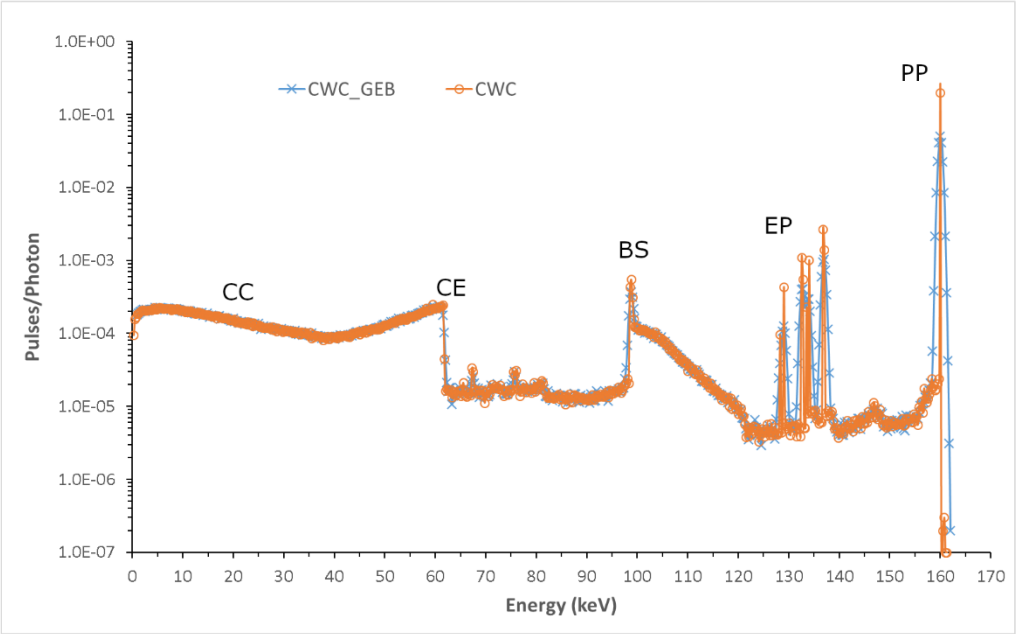


Figures 8-11 show a smoothing of the peaks (PP, EP) and the curves, in a general way, when the GEB card treatment is used. It is also observed some characteristic regions of the spectrum: CC, CE, BS, EP and PP [4]. For photons of higher energies, all these characteristic regions are clearly identified. It's important to highlight the peaks from other adjacent structures of the detector and of the tungsten collimator.

The raw and corrected spectra of qualities N80, N120, W150, W60, and RQR10 normalized by the sum of the counts are shown in Figures 12-16. The spectra were corrected using the C++ program developed in-house [19] along with the response matrices obtained in the CWC, and CWC_GEB simulations. Reference corrected spectra were obtained using the ADMCA software.

**Figure 12:** Comparison of the raw and corrected spectra for the quality N80. Corrected spectra: Reference, CWC and CWC_GEB.

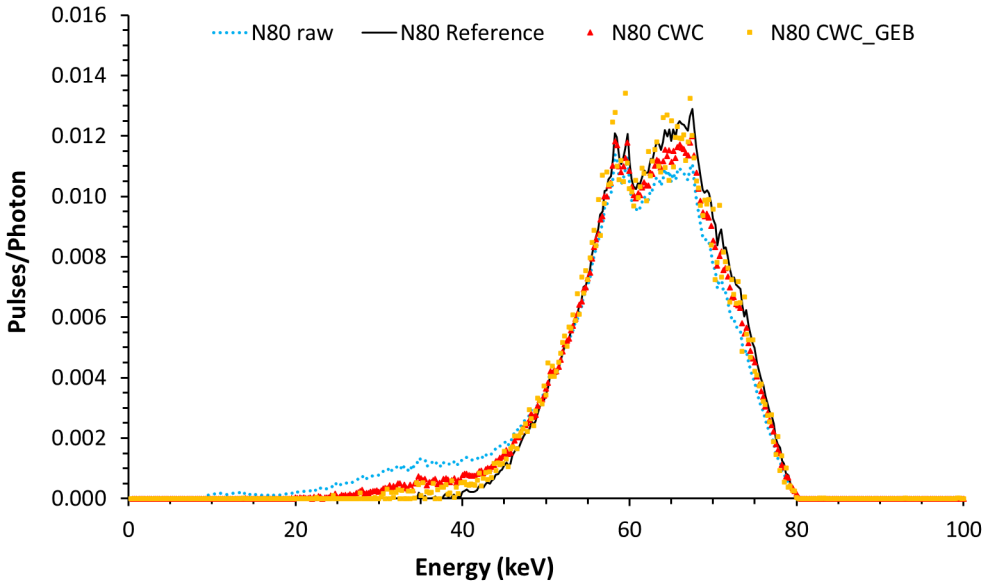


**Figure 13:** Comparison of the raw and corrected spectra for the quality N120. Corrected spectra: Reference, CWC and CWC_GEB.

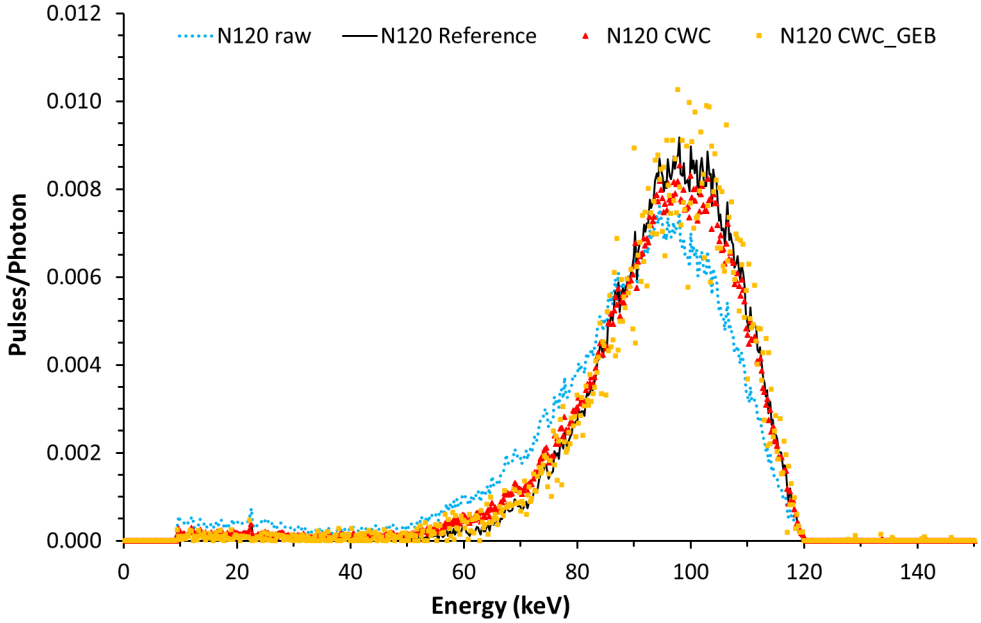

**Figure 14:** Comparison of the raw and corrected spectra for the quality W150. Corrected spectra: Reference, CWC and CWC_GEB.

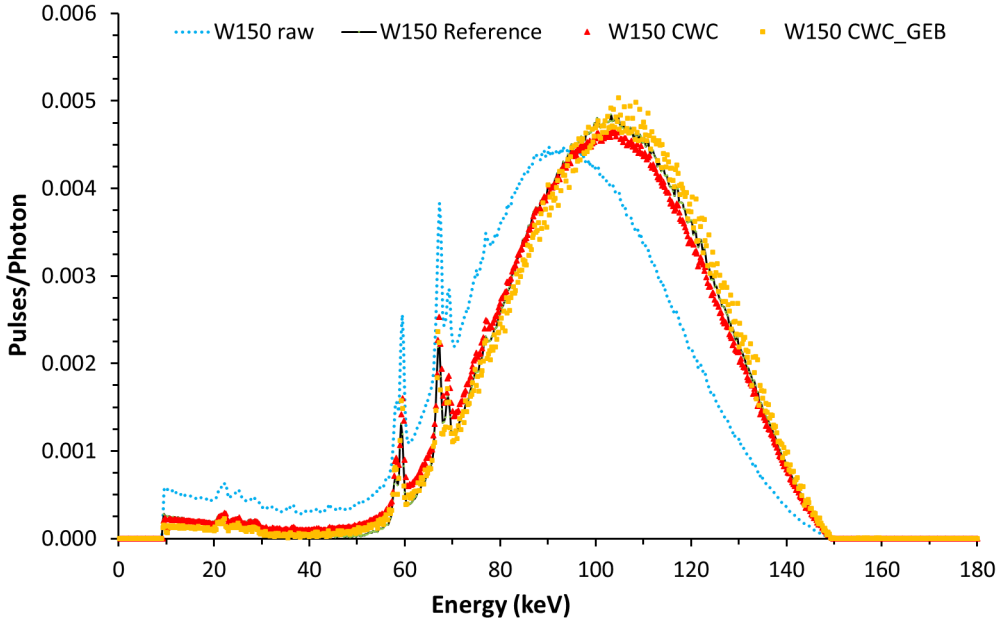


**Figure 15:** Comparison of the raw and corrected spectra for the quality W60. Corrected spectra: Reference, CWC and CWC_GEB.

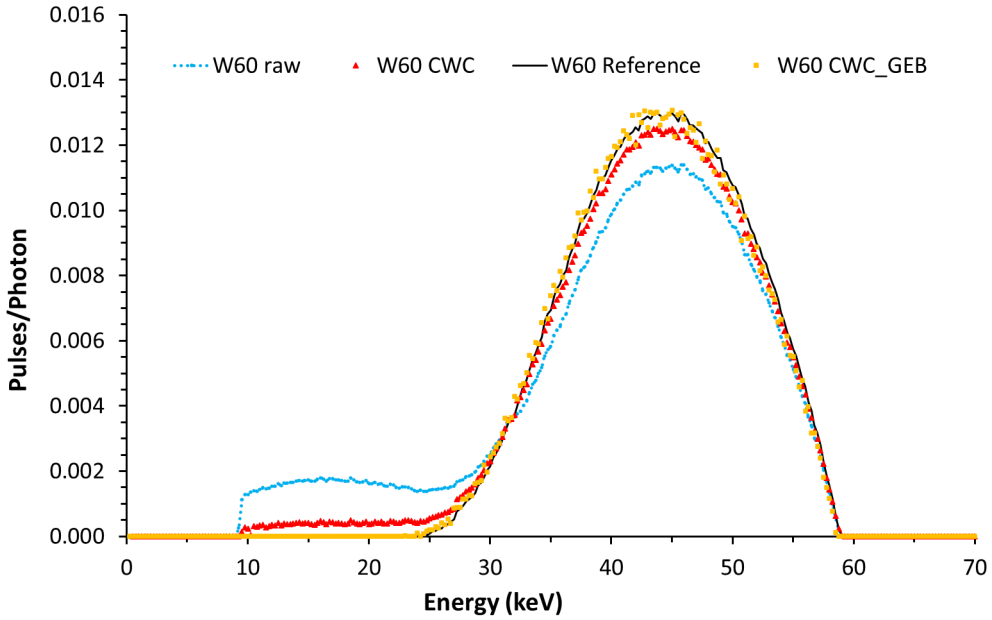

**Figure 16:** Comparison of the raw and corrected spectra for the quality RQR10. Corrected spectra: Reference, CWC and CWC_GEB.

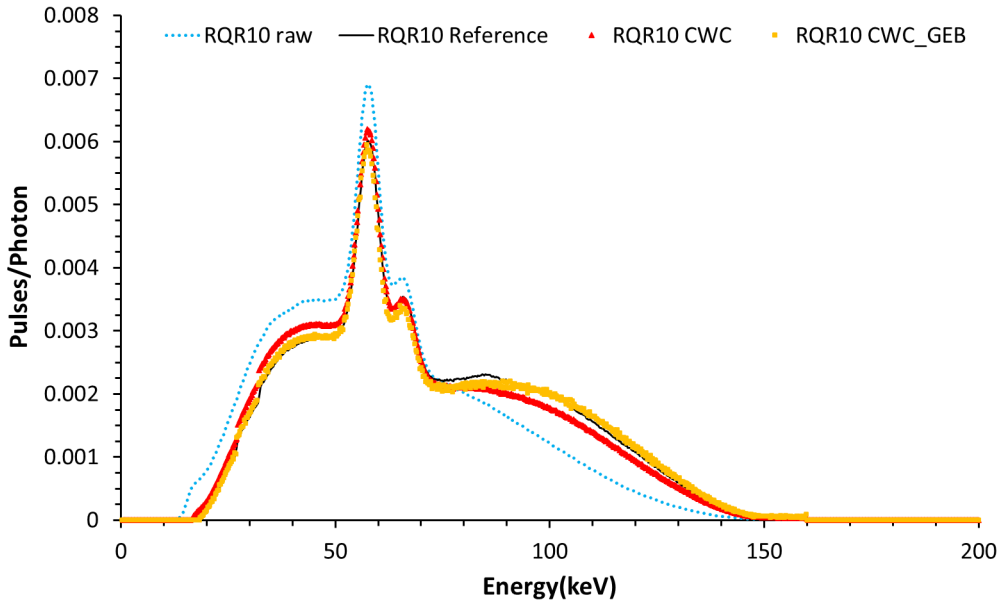


Figures 12-16 show the corrections based on CCC_GEB presented better agreement with the reference spectra. However, the corrections with this matrix, especially for the N80 and N120 spectra, resulted in increased noise in the corrected spectra. This effect was observed to a lesser extent in the spectra of the other qualities.

The ratios CWC/Reference and CWC_GEB/Reference reached values above 10 for some channels. However, for most channels, the ratios were close to 1. The bigest discrepancies occur at the ends of the spectra, especially in the lower energy portion, in which the number of counts is much smaller. The impact of these differences on parameters such as mean energy and HVL of the corrected spectra is not very significant. This fact can be observed in Table 1, which shows a comparison of HVL, Homogeneity Coefficient (HC), and Average Energy values obtained for qualities N80, N120, W150, W60, and RQR10, corrected in the present work using the response matrices CWC, CWC_GEB, and the reference data, obtained with the Reference software [18].

**Table 1 :** Comparison of HVL, Homogeneity Coefficient (HC), and Average Energy values obtained for qualities N80, N120, W150, W60, and RQR10, corrected in the present work using the response matrices CWC, CWC_GEB, and the reference data, obtained with the Reference software [18].

| *Qualities* | 1st HVL mm Al or Cu | 2nd HVL mm Al or Cu | HC | $\bar{E}(\Phi)$ (keV) | Diff. $\bar{E}(\Phi)$ (%) | Diff. HC (%) |
|---|---|---|---|---|---|---|
| **Reference Validated Software (Santos et al., 2017)** | | | | | | |
| N80 | 0.0528 | 0.0566 | 0.9331 | 62.9 | - | - |
| N120 | 0.1455 | 0.1574 | 0.9244 | 94.9 | - | - |
| W150 | 0.1575 | 0.1839 | 0.8564 | 100.6 | - | - |
| W60 | 0.0195 | 0.0222 | 0.8770 | 44.0 | - | - |
| RQR10 | 0.8918 | 1.098 | 0.8122 | 70.8 | - | - |
| **CWC** | | | | | | |
| N80 | 0.0493 | 0.0553 | 0.8908 | 61.4 | -2.3% | -4.4% |
| N120 | 0.1382 | 0.1540 | 0.8970 | 93.1 | -1.9% | -2.9% |
| W150 | 0.1539 | 0.1829 | 0.8417 | 99.9 | -0.7% | -1.8% |
| W60 | 0.0192 | 0.0229 | 0.8377 | 43.7 | -0.6% | -4.5% |
| RQR10 | 0.8437 | 1.061 | 0.7952 | 68.5 | -3.3% | -2.1% |
| **CWC_GEB** | | | | | | |
| N80 | 0.0512 | 0.0561 | 0.9132 | 62.2 | -1.0% | -2.2% |
| N120 | 0.1446 | 0.1579 | 0.9158 | 94.8 | -0.1% | -0.9% |
| W150 | 0.1622 | 0.1880 | 0.8627 | 102.1 | 1.5% | 0.7% |
| W60 | 0.0202 | 0.0231 | 0.8731 | 44.5 | 1.2% | -0.4% |
| RQR10 | 0.9109 | 1.116 | 0.8166 | 71.6 | 1.0% | 0.5% |

Table 1 shows that for the $\bar{E}(\Phi)$ and HC parameters, the response matrix obtained in the CWC_GEB simulations showed the smallest differences in relation to the reference values (-1.0 % to 1.5 %) and (-2.2 % to 0, 7 %) respectively. Differences were less than 5 % considering all evaluated qualities and the two response matrices used in the correction. Based on these results, it can be stated that the correction for finite energy resolution (CWC_GEB) improved the $\bar{E}(\Phi)$ and HC parameters of the corrected spectra compared to

CWC alone. However, a more extensive evaluation, including correction comparisons of a larger number of spectra of different qualities, is still needed to prove these statements

## 4. CONCLUSIONS

In this work, the MCNPX Monte Carlo code was used to study the response functions of a CdTe detector including its collimation system. The detector response functions were obtained and raw spectra were corrected using the response matrices obtained for the detailed modeling of the CdTe (CWC). Differences lower than ± 5 % were observed for $\bar{E}(\Phi)$ and CH parameters using CWC.

The simulations performed using tally F8 coupled to called GEB card (CWC_GEB), considered the energy resolution of the CdTe detector and presented lower differences (< ± 2,5 %) for $\bar{E}(\Phi)$ and HC parameters than the ones obtained using CWC alone. The spectra shape was also in better agreement with the ones corrected with Reference software, however the spectra noise was increased using CWC_GEB, especially for N qualities tested.

The response matrix obtained with the CCC_GEB simulations and the "stripping" methodology used in this work were the best combination to correct x-radiation spectra measured with the CdTe detector, model EXV9 – XR-100T accordind to our results. Future works will focus in the influence of the adjustment parameters of the Gaussian function of the GEB card, in a more extensive validation study with other qualities spectra and in the implementation of corrections for incomplete charge collection and pileup effects.

## ACKNOWLEDGMENT AND FUNDING

Antunes, A.M. wishes to thank the FAPEMIG (Fundação de Amparo à Pesquisa do Estado de Minas Gerais) for the master scholarship. Nogueira, M.S. and Lacerda, M.A.S. are grateful for the financial support provided by FAPEMIG (Fundação de Amparo à Pesquisa do Estado de Minas Gerais) [Projects: Universal Proc. APQ-03290-18 and APQ-01018-21]. This work is part of the Brazilian Institute of Science and Technology for Nuclear Instrumentation and Applications to Industry and Health (INCT/INAIS), CNPq project 406303/2022-3.

## CONFLICT OF INTEREST

All authors declare that they have no conflicts of interest.

## REFERENCES

[1] Kurková, D., Judas, L. X-ray tube spectra measurement and correction using a CdTe detector and an analytic response matrix for photon energies up to 160 keV. **Radiat. Meas.** v.85, p.64-72., 2016.

[2] Miyajima, S., Imagawa, K., Matsumoto, M. CdZnTe detector in diagnostic x-ray spectroscopy. **Med. Phys.** v.29, p.1421–1429, 2002.

[3] Tomal, A., Santos, J.C., Costa, P., Gonzales, A.L., Poletti, M. Monte Carlo simulation of the response functions of CdTe detectors to be applied in x-ray spectroscopy. **Appl. Radiat. Isot.** v.100, p.32-37, 2015.

[4] Knoll, G.F. **Radiation detection and measurement**. Hoboken, NJ: John Wiley & Sons, 2010.

[5] Bonifácio, D.A.B. Validação do Geant4 para a produção e detecção de raios X na faixa de energia de radiodiagnóstico. Dissertação (Mestrado em Física) – Universidade de São Paulo, São Paulo, 2007.

[6] Di Castro, E., Pani, R., Pellegrini, R., Bacci, C. The use of cadmium telluride detectors for the qualitative analysis of diagnostic x-ray spectra. **Phys. Med. Biol.** v.29, 1117, 1984.

[7] Kurková, D., Judas, L. An analytical X-ray CdTe detector response matrix for incomplete charge collection correction for photon energies up to 300 keV. **Radiat. Phys. Chem.** v.146, p.26-33, 2018.

[8] LeClair, R.J., Wang, Y., Zhao, P., Boileau, M., Wang, L., Fleurot, F. An analytic model for the response of a CZT detector in diagnostic energy dispersive x-ray spectroscopy. **Med. Phys.** v.33, p.1329-1337, 2006.

[9] Redus, R.H., Pantazis, J.A., Pantazis, T.J., Huber, A.C., Cross, B.J. Characterization of CdTe detectors for quantitative X-ray spectroscopy. **IEEE Trans. Nucl. Sci.** v.56, p.2524-2532, 2009.

[10] Tomal, A., Cunha, D., Antoniassi, M., Poletti, M. Response functions of Si (Li), SDD and CdTe detectors for mammographic x-ray spectroscopy. **Appl. Radiat. Isot.** v.70, p.1355-1359, 2012.

[11] Seelentag, W., Panzer, W., Drexler, G., Platz, L., Santner, F. A catalogue of spectra for the calibration of dosemeters. Gesellschaft fuer Strahlen- und Umweltforschung m.b.H., Neuherberg (Germany, F.R.). Inst. fuer Strahlenschutz, 1979.

[12] Almeida Jr, A. Caracterização de argamassas de barita como blindagens contra a radiação X e determinação experimental dos coeficientes de atenuação desses materiais, Tese (Doutorado em Engenharia de Materiais) – Universidade Federal de Ouro Preto, Ouro Preto, 2014.

[13] Pelowitz, D.B. MCNPX™ User's Manual, Version 2.7. 0. LA-CP-11-00438. Los Alamos Natl. Lab, United States of America, 2011.

[14] White, M.C. Photoatomic data library MCPLIB03: An update to MCPLIB02 containing Compton profiles for Doppler broadening of incoherent scatteringIntern. Memo. X-5 MCW-02-110 -UR-03-0787, Los Alamos Natl. Lab. United States of America, 2002.

[15] Adams, K. Electron upgrade for MCNP4B. Intern. Memo. X-5-RN U-00-14 May 25, Los Alamos Natl. Lab., United States of America, 2000.

[16] X-5 Monte Carlo Team. MCNP - A General Monte Carlo N-Particle Transport Code, Version 5. LA-UR-03-1987, Los Alamos Natl. Lab., United States of America, 2008.

[17] Stankovic, J., Marinkovic, P., Ciraj-Bjelac, O., Kaljevic, J., Arandjic, D., Lazarevic, D. Toward utilization of MCNP5 particle track output file for simulation problems in photon spectrometry. **Comput. Phys. Commun.** v.195, p.77-83, 2015.

[18] Santos, J.C., Tomal, A., Furquim, T.A., Fausto, A.M., Nogueira, M.S., Costa, P.R. Direct measurement of clinical mammographic x-ray spectra using a CdTe spectrometer. **Med. Phys.** v.44, p.3504-3511, 2017.

[19] Mendes, B.M., Squair, P.L., Figueiredo, M.T.T., Nogueira, M.S., 2018. Development of a methodology for CdTe detector spectra correction using MCNPx simulations, in: 14th International Symposium on Radiation Physics. Presented at the ISRP-14. 14th International Symposium on Radiation Physics, Córdoba.

[20] R. Kunzel, Herdade, S.B., Terini, R.A., Costa, P.R. X-ray spectroscopy in mammography with a silicon PIN photodiode with application to the measurement of tube voltage. **Med. Phys.** v.31, p.2996-3003, 2004.

[21] Berger, M., Hubbell, J., Seltzer, S., Chang, J., Coursey, J., Sukumar, R., Zucker, D., Olsen, K., 2010. XCOM: photon cross section database (version 1.5),[Online] Available: http://physics. nist. gov/xcom, National Institute of Standards and Technology, Gaithersburg. Gaithersburg MD.

## LICENSE